Manuscript prepared for Atmos. Chem. Phys.
with version 3.2 of the LaTeX class copernicus.cls.
Date: 26 August 2011

Laboratory studies of the chemical composition and cloud condensation nuclei (CCN) activity of secondary organic aerosol (SOA) and oxidized primary organic aerosol (OPOA)

A. T. Lambe[1,2], T. B. Onasch[1,2], P. Massoli[2], D. R. Croasdale[1], J. P. Wright[1], A. T. Ahern[1,2], L. R. Williams[2], D. R. Worsnop[2], W. H. Brune[3], and P. Davidovits[1]

[1]Chemistry Department, Boston College, Chestnut Hill, MA, USA
[2]Aerodyne Research Inc., Billerica, MA, USA
[3]Department of Meteorology and Atmospheric Sciences, The Pennsylvania State University, State College, PA, USA

1 Supporting Information

1.1 laboratory SOA and OPOA precursors

Figure S1 shows molecular structures for twelve of the fourteen precursors studied in the present work; diesel fuel and 10W-30 engine lubricating oil are not shown. As discussed in Section 2.3, SOA particles were generated via gas-phase oxidation of volatile organic compounds (VOCs) and intermediate-volatility organic compounds (IVOCs) in the PAM reactor. The VOC precursors used in this study were *n*-decane (*n*-C_{10}), isoprene, α-pinene, β-pinene, toluene, m-xylene, and mesitylene. The IVOC precursors used in this study were *n*-heptadecane (*n*-C_{17}), diesel fuel, longifolene, and naphthalene. Table S1 shows VOC precursor mixing ratios that were used in this work; IVOC precursor mixing ratios were not measured.

OPOA was generated by heterogenous oxidation of bis(2-ethylhexyl) sebacate (BES) and 10W-30 engine lubricating oil particles. Another set of experiments was conducted with an internally mixed primary aerosol composed of glyoxal and ammonium sulfate.

1.2 SOA size distributions

Figure S2 shows representative SMPS volume distributions of SOA generated from α-pinene and naphthalene in the PAM reactor. Volume distributions are normalized to compare changes in particle size as a function of OH exposure; data shown ranges from 1.6×10^{11} molec cm^{-3} s to 2.1×10^{12} molec cm^{-3} s. The slight increase in volume at $D_m \approx 300$ nm corresponds to doubly-charged particles that are misclassified by the DMA. In general, for SOA generated from a specific precursor, the SMPS volume distribution trends toward smaller sizes with increasing OH exposure. This might correspond to fragmentation and/or changes in volatility of the SOA. In most cases, the effective density of the SOA is in the range of 1.2 – 1.6 g cm^{-3} as determined from SMPS and AMS measurements.

Correspondence to: A. T. Lambe
(andrew.lambe@bc.edu)

1.3 lower limits of κ_{org} for SOA and OPOA

The lower-limit κ_{org}-values are a function of the dry diameter selected for CCN analysis, which ranged from 45 to 150 nm for SOA and 145 to 200 nm for OPOA, as well as the maximum water vapor supersaturation attainable with the CCNC (1.5% in the present work). Figure S3 shows the lower limits of κ_{org} as a function of particle mobility diameter. These κ values were taken from a κ-lookup table at http://www4.ncsu.edu/∼mdpetter/code.html, which specifies theoretical κ values ranging from 1×10^{-6} to 1 for particle diameters ranging from 10 to 1000 nm. However, the measured lower limit of κ may be affected by trace contaminants that are hygroscopic. For example, a conservative estimate of the ToF-AMS detection limit (defined here as 3 × standard deviation of measured HEPA-filtered AMS signal) is about 60 ng m^{-3}. If 60 ng m^{-3} of water-soluble contaminant (κ = 0.1 - 1) were mixed with an insoluble organic compound (κ = 0) at organic aerosol concentrations ranging from 10 100 μg m^{-3} (typical range of POA mass loadings that was used), measured κ-values could be as low as 6×10^{-6} and as high as 6×10^{-4} . From these calculations, we estimate a conservative lower limit of κ_{org} = 6×10^{-4}. Figure S4 shows the corresponding (red) and theoretical lower-limit (grey) κ_{org}-values as a function of O/C ratio for SOA/OPOA generated in the PAM reactor. A dashed line at κ = 6×10^{-4} is also shown to represent the experimental lower limit of κ. Likewise, upper-limit (black) κ_{org}-values are shown for unoxidized BES and lubricating oil particles. In this case, κ_{org} $< 6\times10^{-4}$ for the unoxidized POA.

1.4 thermally denuded PAM-generated SOA

In a subset of experiments, an Aerodyne thermal denuder (Huffman et al., 2008) was placed upstream of the AMS and SMPS to investigate the chemical composition of PAM-generated SOA as a function of organic aerosol concentration. The heated section of the thermal denuder was set to several constant temperatures (T = 60- 250^{o}C) and allowed to equilibrate before measurements. Combined flows through the thermal denuder ranged between 2 - 3 lpm, corresponding to residence times of 3-5 sec and 3-4 sec in the heater and denuder sections, respectively. Figure S5 shows f_{44} versus f_{43} for thermally denuded SOA generated from naphthalene and α-pinene oxidation in the PAM reactor. As is evident, thermally denuding the aerosol increases f_{44} and decreases f_{43}. At a specific OH exposure, f_{44} of α-pinene SOA increased by 12% - 26% as a function of thermal denuding, accompanied by a 15% - 33% decrease in f_{43}. Likewise, the f_{44} of naphthalene SOA increased by 6% - 232%, accompanied by a 12% - 17% decrease in f_{43}. Similar trends were observed by lowering the SOA precursor concentration that was input to the PAM reactor. These results are consistent with OOA at *m/z*=43 and *m/z* = 44 representing semivolatile and low-volatilty organics, respectively.

1.5 AMS spectra of PAM-generated SOA at low and high OH exposures

Figures S6, S7, and S8 show AMS spectra of SOA generated from the oxidation of alkane, terpenoid, and aromatic precursors respectively. We used the ToF-AMS fragmentation table coefficients recommended by Aiken et al. (ES&T, 2008) for organic signal apportionment at *m/z* = 16 - 20 and 28 (e.g. frag_organic[18] = 0.225× frag_organic[44] and frag_organic[28] = frac_organic[44]). Spectra are shown for low (1.6×10^{11} molec cm^{-3} s) and high (2.2×10^{12} molec cm^{-3} s) OH exposures in the PAM reactor, except for isoprene SOA, for which AMS spectra are shown at 1.6×10^{11} molec cm^{-3} s and 1.0×10^{12} molec cm^{-3} s. The overall complexity of the AMS spectra decreases at high OH exposure conditions. This is presumably because oxidation converts the lesser-oxidized compounds to products that contribute to *m/z* = 44 and related peaks, namely m/z = 18 and 28, such as carboxylic acids. Accordingly, AMS spectra of SOA generated at high OH exposures are mostly similar, with the exception of SOA generated from isoprene.

However, the AMS spectra at low OH exposures vary significantly over the range of precursors. This reflects the wide range of precursor structures. Spectra of SOA generated from alkanes (Fig. S6) reveal "picket-fence" fragmentation patterns at alkyl peaks characteristic of hydrocarbon-like organic aerosol (HOA; e.g. *m/z* = 41, 43, 55, 57, 67, 69, 71). In addition, there are significant contributions at peaks representative of oxygenated organic aerosol (OOA; e.g. *m/z* = 44) and other smaller ions (e.g. *m/z* = 26, $C_2H_2^+$). Further, HR-ToF-AMS measurements reveal that in some cases oxygenated ions contribute significantly to peaks normally associated with HOA, even at low OH exposures. One example is shown in Fig. S11 for signal at *m/z* = 57 in C_{17} SOA generated at an OH exposure of 1.6×10^{11} molec cm^3 s. Fig. S11 also shows that signal at *m/z* = 44 for C_{17} SOA generated at low OH exposure contains a significant fraction of $C_2H_4O^+$ ions, whereas the *m/z* = 44 signal in most types of SOA is predominately CO_2 ions. Similar features were observed for SOA generated from C_{10} and diesel fuel, as discussed in Section 3.1 and shown in Fig. 3.

Spectra of SOA generated from terpenoids (Fig. S7) and aromatics (Fig. S8 are more diverse at low OH exposures. For example, spectra for SOA generated from lower-molecular weight precursors (e.g. isoprene, toluene) have signal predominately at *m/z* < 60. On the other hand, SOA generated from longifolene and from naphthalene have significant peaks at *m/z* > 100, which may indicate oxidation products retaining cyclic structure of their respective precursors.

1.6 PAM-generated SOA containing f_{43} curvature

Figure S9 shows f_{44} as a function of f_{43} for SOA generated from nine of the fourteen precursors in the PAM reactor. These SOA systems were characterized by increases and subsequent decreases in f_{43} with oxidation, suggesting the formation and decay of early-generation oxidation products containing high f_{43} (specifically, $C_2H_3O^+$ ions).

1.7 O/C-f_{44} and H/C-f_{43} of PAM-generated SOA

Figures S10a and S10b shows O/C ratio as a function of f_{44} and H/C ratio as a function of f_{43} for PAM-generated SOA and OPOA. The dashed line Fig. S10a (O/C = 3.82×f_{44} + 0.0794) is the best fit to multiple laboratory and field datasets (Aiken et al., 2008). The black dashed line in Fig. S10b (H/C = 1.01 + 6.07×f_{43} - 16.01×$f_{43}{}^2$) is a quadratic fit to smog chamber and field data (Ng et al., 2011b); grey dashed lines represent 10% confidence intervals to the quadratic fit as presented by Ng et al.

Table S1. SOA precursor mixing ratios ("ND" = not determined)

Precursor	Mixing Ratio (ppbv)
n-C_{10}	102 – 330
n-C_{17}	ND
diesel fuel	ND
isoprene	330
α-pinene	40 – 80
β-pinene	50
longifolene	ND
toluene	80
m-xylene	90 – 100
mesitylene	120 – 150
naphthalene	ND

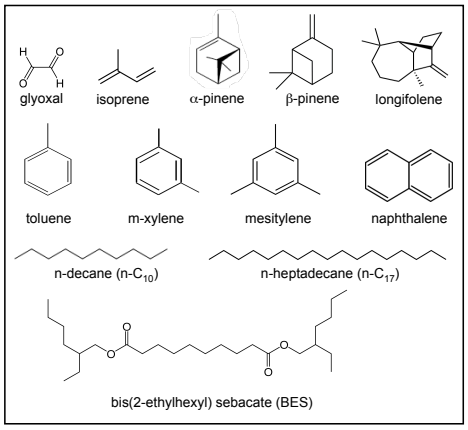

Fig. S1. Molecular structures of gas- and condensed-phase oxidized organic aerosol precursors used in this study.

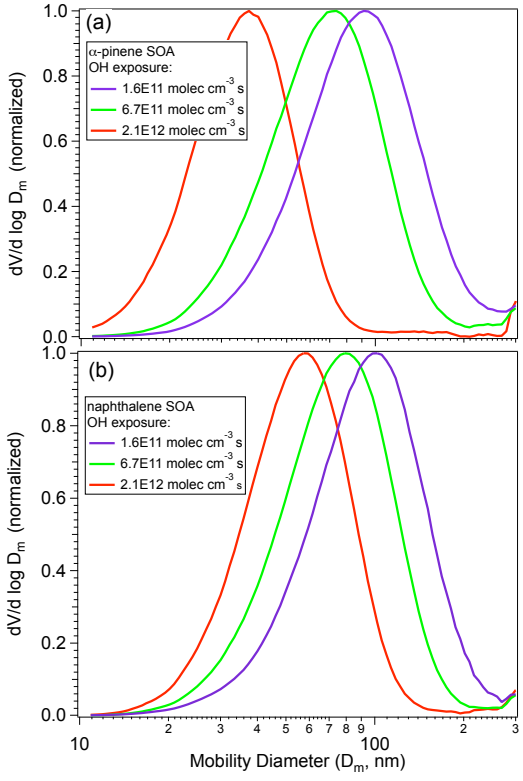

Fig. S2. Normalized SMPS volume distributions of SOA generated in the PAM reactor from (a) α-pinene and (b) naphthalene at "low", "medium", and "high" OH exposures.

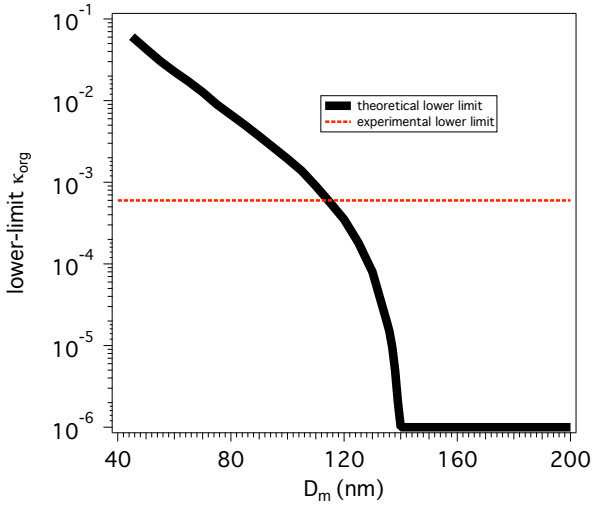

Fig. S3. Lower-limit κ-org values as a function of mobility diameter (D_m). Values are taken from κ_{app}-lookup table at http://www4.ncsu.edu/∼mdpetter/code.html and correspond to a critical supersaturation of 1.5%. For details see text.

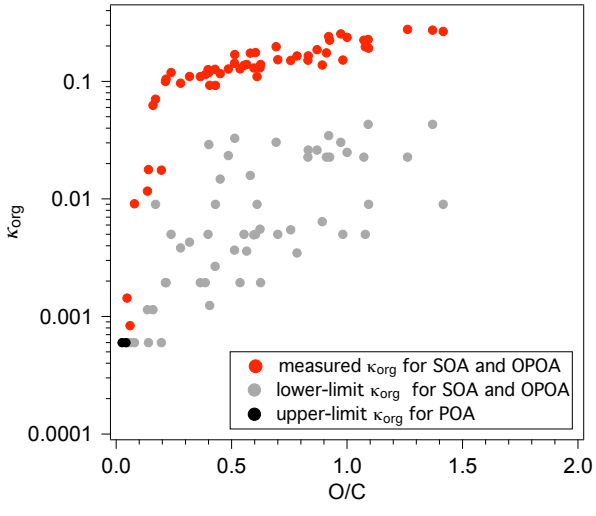

Fig. S4. Measured (red) and lower-limit (grey) κ-org values as a function of O/C ratio for SOA and for OPOA . Upper-limited values for unoxidized POA (black) are also shown. For details see text.

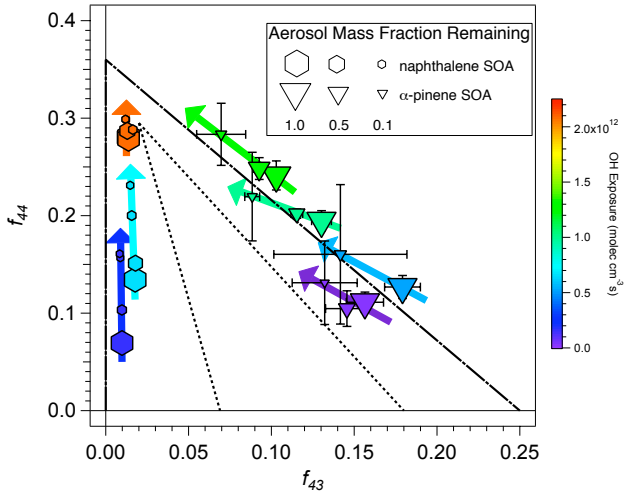

Fig. S5. f_{44} shown as a function of f_{43} for thermally denuded naphthalene and α-pinene SOA. Symbols are colored by OH exposure in the PAM reactor and sized by aerosol mass fraction remaining (relative to non-denuded conditions). Error bars represent $\pm 1\sigma$ in measurements. Dashed lines indicate range of ambient f_{44} and f_{43} measurements, while dashed-and-dotted lines indicate range of laboratory PAM reactor measurements.

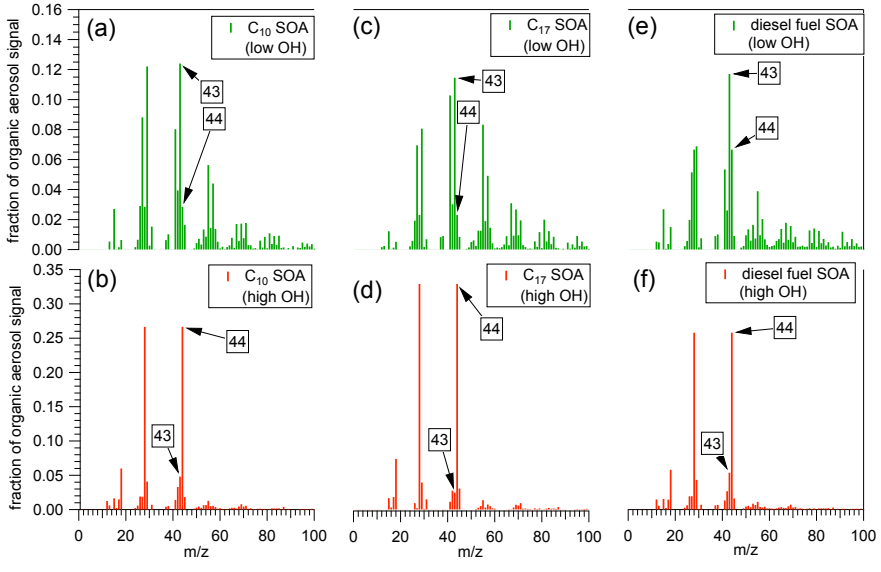

Fig. S6. AMS spectra of SOA generated from oxidation of (a, b) C_{10}, (c, d) C_{17}, and (e, f) diesel fuel at low and high OH exposures in the PAM reactor (1.6×10^{11} and 2.2×10^{12} molec cm^{-3} s respectively).

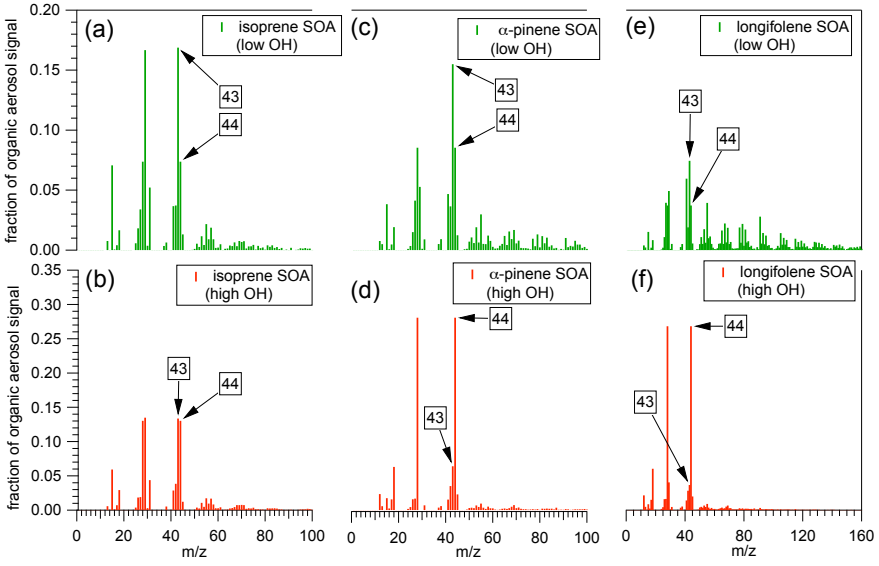

Fig. S7. AMS spectra of SOA generated from oxidation of (a, b) isoprene, (c, d) α-pinene, and (e, f) longifolene at low and high OH exposures in the PAM reactor (1.6×10^{11} and 2.2×10^{12} molec cm^{-3} s respectively, except for mass spectra of isoprene SOA which are shown at OH exposures of 1.6×10^{11} and 1.0×10^{12} molec cm^{-3} s). AMS spectra of longifolene SOA are shown up to m/z = 160 to display prominent fragments at m/z $>$ 100.

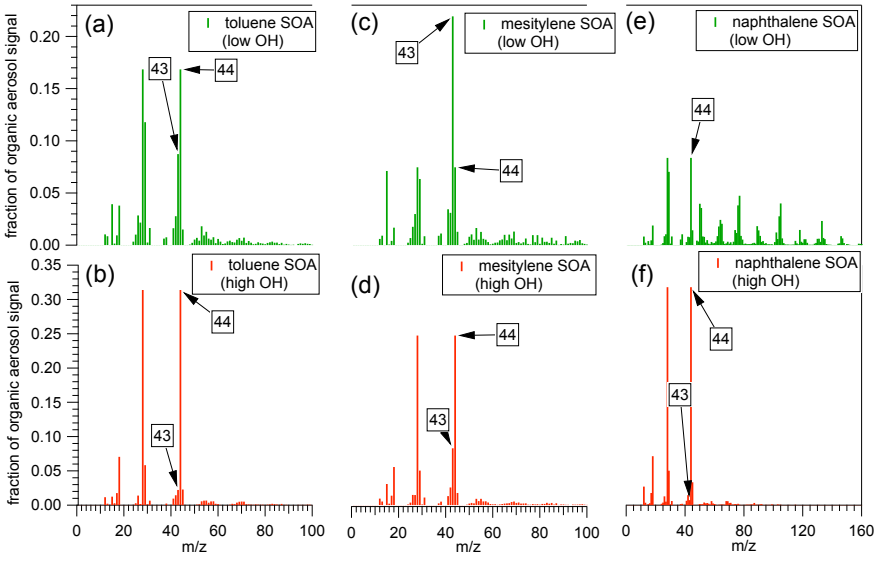

Fig. S8. AMS spectra of SOA generated from oxidation of (a, b) toluene, (c, d) mesitylene, and (e, f) naphthalene at low and high OH exposures in the PAM reactor (1.6×10^{11} and 2.2×10^{12} molec cm^{-3} s respectively). AMS spectra of naphthalene SOA are shown up to m/z = 160 to display prominent fragments at m/z $>$ 100.

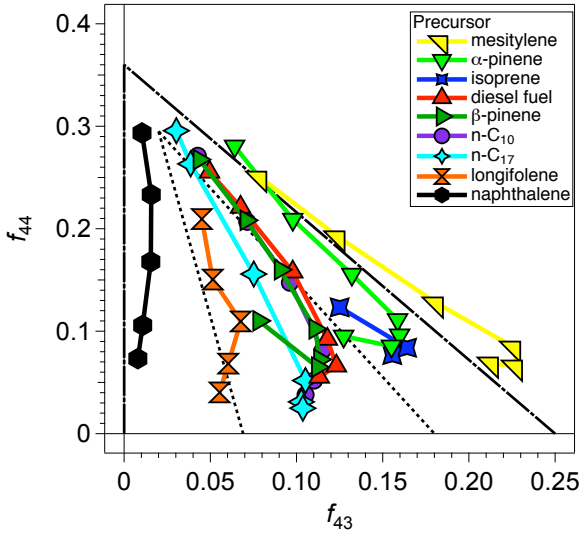

Fig. S9. f_{44} shown as a function of f_{43} for PAM-generated SOA characterized by f_{44}–f_{43}-curvature (replotted from Fig. 2). Dashed lines indicate range of ambient f_{44} and f_{43} measurements, while dashed-and-dotted lines indicate range of laboratory PAM reactor measurements.

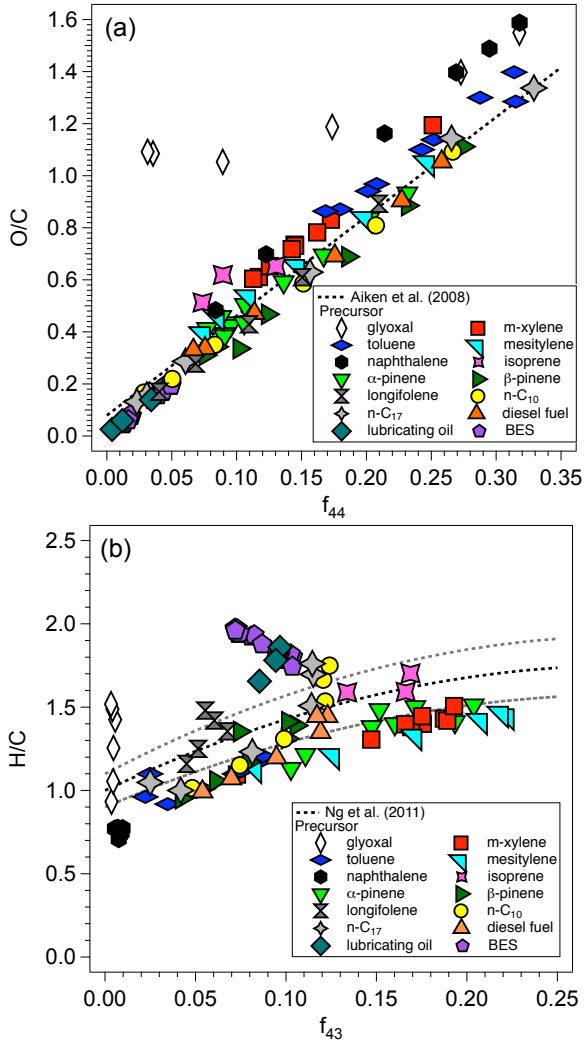

Fig. S10. (a) Oxygen-to-carbon (O/C) ratio as a function of f_{44} and (b) hydrogen-to-carbon (H/C) ratio as a function of f_{43} for PAM-generated SOA and OPOA. Dashed lines represent O/C-f_{44} and H/C-f_{43} parameterizations from Aiken et al. (2008) and Ng et al. (2011b) respectively. Glyoxal OPOA (diamonds) deviates from Aiken et al. and Ng et al. parameterizations for reasons described in the text.

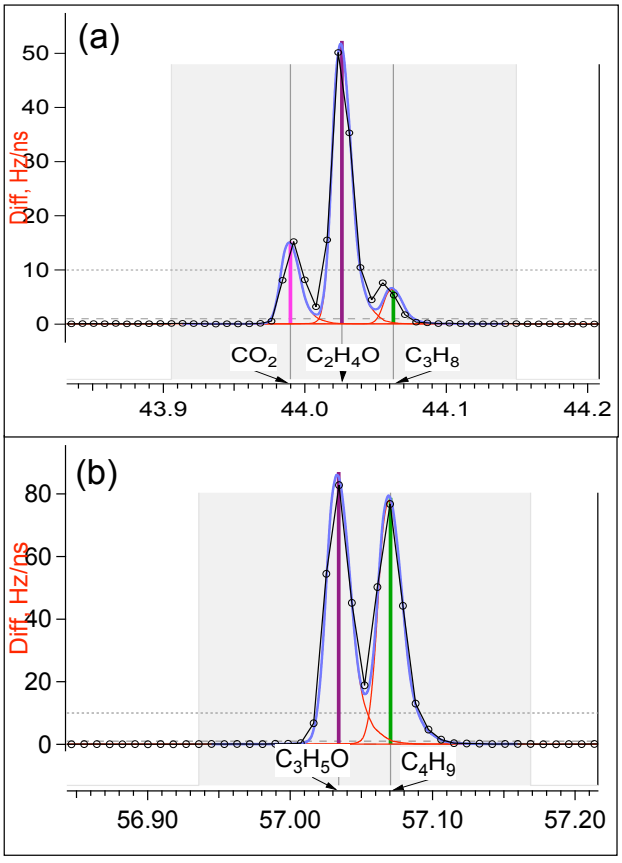

Fig. S11. HR-ToF-AMS ion signals at (a) *m/z* = 44 and (b) *m/z* = 57 for SOA generated from n-C_{17} at an OH exposure of 1.6×10^{11} molec cm^{-3} s. Background-corrected "difference" signals are shown.